Annales Geophysicae, 23, 2295–2305, 2005
SRef-ID: 1432-0576/ag/2005-23-2295

Annales Geophysicae

SEEK-2 (Sporadic-E Experiment over Kyushu 2) – Project Outline, and Significance

M. Yamamoto[1], **S. Fukao**[1], **R. T. Tsunoda**[2], **R. Pfaff**[3], **and H. Hayakawa**[4]

[1]Research Institute for Sustainable Humanosphere, Kyoto University, Uji, Kyoto, Japan
[2]Center for Geospace Studies, SRI International, Menlo Park, CA, USA
[3]NASA/Goddard Space Flight Center, Greenbelt, MD, USA
[4]Institute of Space and Aeronautical Science, Japan Aerospace Exploration Agency, Sagamihara, Kanagawa, Japan

Received: 8 February 2005 – Revised: 14 June 2005 – Accepted: 12 July 2005 – Published: 13 October 2005

Part of Special Issue "SEEK-2 (Sporadic-E Experiment over Kyushu 2)"

Abstract. SEEK-2 (Sporadic-E Experiment over Kyushu 2) is an observation campaign to study the spatial structure of the field-aligned irregularity (FAI) and sporadic-E(E_s)-layer by means of two sounding rockets and a ground-based observation network with radars and optical instruments. The experiment was successfully conducted on 3 August 2002, with successive launches of two sounding rockets from the Uchinoura Space Center (USC) of the Japan Aerospace Exploration Agency (JAXA). The timing of the experiment was carefully selected, while intense quasi-periodic (QP) echoes were observed with two radars in Tanegashima. The main E_s-layer, with its double-layered structure, was observed at altitudes of 103–105 km, the presence of which was well accounted for by the ion accumulation due to neutral-wind shear. Several minor peaks were detected in the electron density profiles at altitudes of up to 130 km. The intensity of the electric field was 5–10 mV/m and showed intense fluctuations below 110 km. Wave-like variation of the electric field was seen above 110 km. From radar experiments, we found that QP echoes appeared around 105 km, which agreed well with the main E_s-layer height. The QP echoes propagated to the west-northwest, with frontal structures elongated from north-northeast to south-southwest. Radar observations conduced throughout the SEEK-2 period, on the other hand, showed that frontal structures of the QP echoes were most frequently propagated to the southeast. This result was consistent with the direction of gravity-wave propagation observed with the OH imager during the same period. The rocket beacon experiment with the E_s-layers revealed the spatial structure of the plasma densities. On the basis of these results and those from SEEK-1 in 1996, we examined the structures of the nighttime mid-latitude E-region. We concluded that the QP echoes reflect the horizontal structures of the main E_s-layers. The source of the structures was not clearly determined from the experiments, but the candidates are gravity waves and the Kelvin-Helmholtz instability. The azimuth-dependent E_s-instability may have contributed to enhance structures of the QP echoes, although this instability may not be a major source of the QP structure in SEEK-2. Polarization electric fields were induced from the E_s-layer with QP echoes, mapped upward along the geomagnetic field, and played an important role in determining the structures of the whole ionospheric E-region.

Keywords. Mid-latitude ionosphere – Ionospheric irregularities – Ionosphere-atmosphere interactions

1 Introduction

This paper presents the project outline of the Sporadic-E Experiment over Kyushu 2 (SEEK-2) and a summary of its experimental results. SEEK-2 is an experimental campaign with sounding rockets and ground-based instruments for investigations of structures of the mid-latitude E-region that consists of interesting physical phenomena, i.e. sporadic E(E_s)-layers and ionospheric field-aligned irregularities (FAIs). In the mid-latitude E-region after sunset, we can find intense radar backscatter echoes from FAIs perpendicular to the geomagnetic field. From this perpendicularity, their Doppler spectral characteristics, and association with E_s-layers, the FAI echoes are explained by Bragg scattering from the gradient-drift instability that appears at intense plasma-density gradient of the E_s-layers. An interesting feature of the backscatter echoes is that they sometimes show 5–10 min periodicity with (mostly) incoming phase propagation. These phenomena are called quasi-periodic (QP) echoes. The QP echoes were first clearly observed by the MU radar in Japan (Fukao et al., 1991; Yamamoto et al., 1991, 1992), although they were vaguely detected in earlier radar observations (Ecklund et al., 1981; Tanaka and Venkateswaran, 1982; Riggin et al., 1986). Since wave-like characteristics of the QP echoes resembled those of gravity waves, the generation mechanism of the QP echoes was not attributed to plasma instabilities. The association of the QP echoes with E_s-layers was first explained by large height

modulation of E_s-layers by gravity waves (Woodman et al., 1991; Tsunoda et al., 1994).

Based on these earlier studies of the QP echoes, the first SEEK (Sporadic-E Experiment over Kyushu; hereafter we refer to it as SEEK-1) campaign was conducted in August 1996 in Japan (Fukao et al., 1998). It was designed to measure small-scale electrodynamic perturbations of the E-region by the in-situ instruments on two sounding rockets while the QP echoes were observed by a ground radar. The experiments were successful, and we obtained the following results:

1. The association of QP echoes with E_s-layers was confirmed by the simultaneous rocket/radar experiment (Yamamoto et al., 1998; Tsunoda et al., 1998a).
2. Electric field intensities of 10–20 mV/m were observed in the QP echo region (Pfaff et al., 1998; Nakamura et al., 1998; Yamamoto et al., 1998).
3. E_s-layers were generated by an intense neutral wind shear, which was found to be highly unstable (Larsen et al., 1998).
4. Deep height modulation of E_s-layers was not recognized by two sounding rocket experiments conducted on separate nights (Fukao et al., 1998).
5. Several minor density peaks were found above the major E_s-layers (M.-Y. Yamamoto et al., 1998).
6. The wave-like structure of the electric field above 120 km implied gravity-wave modulation of the polarization electric field (Pfaff et al., 1998).

These results from SEEK-1 denied the existence of deep E_s-modulation and earlier QP-echo models. Instead, two different mechanisms were proposed after these findings. One regarded the large polarization electric field as a key feature to be explained. The possible generation mechanism of the large electric field in the mid-latitude E_s-layer was first proposed by Haldoupis et al. (1996) from the discovery of mid-latitude "type-1" echoes over Crete. Tsunoda (1998b) modified the model to fit the QP echoes, assuming a slab-like enhancement of E_s-layer plasma along the geomagnetic field, and showed that a polarization electric field would form when ambient electric fields or neutral winds were applied. Maruyama et al. (2000) showed a more realistic model that assumed a background E-region plasma and an E_s-layer with plasma-density enhancement. The model explains the generation of the polarization electric field, the existence of the field-aligned current, and the generation of FAIs with QP structures. Another type of model concerned the existence of intense wind shear with E_s-layer that possibly induces shear instability. Larsen (2000) proposed the Kelvin-Helmholtz instability (KHI) as a possible seeding mechanism for the QP echoes and posited that each billow of the KHI wave could be associated with the QP structure.

In most of the radar observations, spectral shapes of the mid-latitude FAI echoes are categorized as "type 2", for which the gradient-drift instability is expected. In the very simple theory, the gradient-drift instability can increase when the electric field is parallel to the sharp density gradient of an E_s-layer. In the mid-latitude region, however, a confounder was pointed out: The instability at one side of the E_s-layer would be suppressed by the stable condition on the other side through the electric-field mapping effect along the inclined geomagnetic field (e.g. Woodman et al., 1991). Recently, careful studies were conducted on this electric field-mapping effect of the mid-latitude gradient-drift instability (Rosado-Roman et al., 2004; Seyler et al., 2004). From nonlocal linear theory of the instability, it was found that ambient electric field strengths of a few millivolts per meter are sufficient to excite the gradient-drift waves associated with an E_s-layer (Seyler et al., 2004). It is suggested that with a gradient length of 250 m and an electric field intensity of 3 mV/m, the wavelength of the fastest growing mode is about 24 m (Rosado-Roman et al., 2004). A theoretical study by Kagan and Kelley (1998) proposed that the gradient-drift instability could be induced by the neutral winds at both upper and lower density gradients when an E_s-layer is generated by zonal wind shear. This wind-driven instability mechanism was also supported by the result of the above-mentioned nonlocal consideration of the gradient-drift instability.

There are several simulation studies concerning the mid-latitude E-region. Generation of the polarization electric field was studied by Yokoyama et al. (2003, 2004a). They conducted two- and three-dimensional simulations and showed that, by applying an ambient electric field or neutral wind to spatially structured E_s-layers, a polarization electric field of several millivolts per meter can be induced. Their new finding was that the induced electric fields propagate along the field line and generate a secondary plasma density gradient above the E_s-layer. They also showed that the F-region plasma density largely controls the E-region electric field and its field-aligned mapping. Cosgrove and Tsunoda (2002, 2003) proposed a new instability mechanism that increases in the mid-latitude E-region. The mechanism resembles the Perkins instability (Perkins, 1973) and can grow when altitude modulation of an E_s-layer has a phase front from northwest to southeast. For KHI seeding mechanisms of the QP echoes, Bernhardt (2002) simulated E_s-layer modulation by means of neutral-air motion associated with the KHI. He showed that the E_s-layer is modulated along the envelope of the KHI billows around 100 km, while the KHI can generate plasma-density enhancement at 120 km.

After SEEK-1 there were many reports addressing the QP structures in the FAIs, not only from Japan or Taiwan but also from different locations, including the low-latitude regions (e.g. Tsunoda et al., 1999; Hysell and Burcham, 2000; Chau et al., 2002; Fukao et al., 2003). Low-altitude QP (LQP) echoes that appear below 100 km are found from Japan, India, and Puerto Rico (Rao et al., 2000; Pan and Rao, 2002; Urbina et al., 2000; Ogawa et al., 2002), also. QP structures themselves are now regarded as a general feature that appear in the E-region FAIs, although their generating mechanisms might vary by case. In terms of the spatial structure

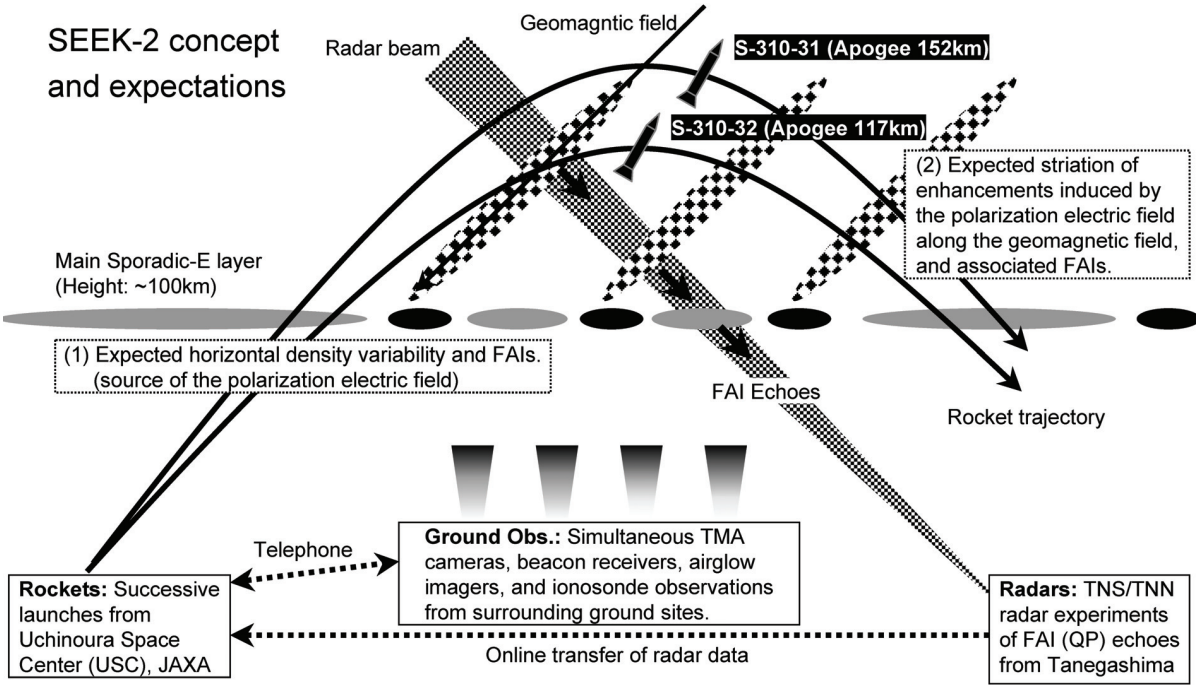

Fig. 1. SEEK-2 experiment. We planned to launch two sounding rockets, S-310-31 and S-310-32, into the region with intense FAI echoes detected by two portable radars in Tanegashima. Horizontal structures of an E_s-layer and field-elongated structure of the E-region plasma were expected from several studies before the experiment, which was based on Fig. 9 of Ogawa et al. (2002).

of the QP echoes, Hysell et al. (2002) conducted radar imaging of FAI echoes with the MU radar and reported that they were attributed to the horizontal structures of the E_s-layers. From earlier MU radar interferometry observations, on the other hand, Yamamoto et al. (1994) reported that FAI echoes can reach the altitude of 120 km. Concerning the relationship with the background E-region conditions, Ogawa et al. (2002) conducted ionosonde observations of E_s-layers simultaneously with the MU radar. They reported that the FAI echoes appear when $\Delta f = f_o E_s - f_b E_s$ exceeds 1 MHz and that their echoes are enhanced with increasing Δf. This finding suggests that the FAIs are generated in association with the enhanced spatial structure of the E_s-layers. SEEK-2 was planned based on the results from SEEK-1 and following studies on the QP-echo mechanisms described above. Figure 1 shows the concept of the SEEK-2 experiment. We planned to monitor FAI echoes in the E-region from separate radar sites and then launch sounding rockets for in-situ observations. This figure also includes expected results from the schematic view of the QP echoes and the E_s-layer structures by Ogawa et al. (2002). While planning the SEEK-2 experiment, we postulated that there is a horizontally structured E_s-layer that induces polarization electric fields, as well as field-elongated plasma enhancements generated by the electric fields above it. FAIs were expected at the edges of both the main E_s-layer and field-elongated plasma structures. We note that SEEK-2 was conducted during the solar-maximum period, while SEEK-1 was in the solar-minimum period. Keeping in mind the basic concept of SEEK-1, we tried to advance the experiment by launching two rockets as close as possible in time. We tried with both rockets to measure plasma density. We introduced a dual-band beacon experiment in both rockets to measure the horizontal structure of E_s-layers. On the ground, we used two radars to measure FAIs, instead of one radar in SEEK-1. One of the radars in SEEK-2 had radio interferometry capability for correct measurements of spatial structures of the QP echoes. The rocket experiments on 3 August 2002 were successful. In this paper, we describe the experimental setup of SEEK-2 and summarize the results, and we discuss structures of E_s-layers and possible mechanisms that generate the QP echoes.

2 Experimental setup and operation

SEEK-2 was conducted in the region shown in Fig. 2. The main part of the experiment was to launch two sounding rockets into E_s-layers while intense FAI echoes were observed from the region of the rocket experiment. We installed ground-based instruments around the rocket range, as listed in Table 1. The rocket experiments were conducted by the Institute of Space and Aeronautical Science, Japan Aerospace Exploration Agency (ISAS/JAXA), from Uchinoura Space Center (USC). We used two single-stage sounding rockets, S-310-31 and S-310-32, that were outfitted with instruments, as listed in Table 2. Two rocket launches were planned 15 minutes apart. On both rockets, an electron density profile was measured using impedance probes (NEI). We installed a fixed-bias probe (FBP) with S-310-31

Table 1. Observation sites and ground-based instruments in SEEK-2. Site locations are shown in Fig. 2.

Site No.	Instrument	Institute
1	Lower-Thermosphere Profiler Radar (LTPR)	Kyoto Univ.
2	Frequency Agile Radar (FAR)	Kyoto Univ., NiCT, and NCU
8	Ionosonde	NiCT
2, 4, 7	Airglow imagers	Nagoya Univ. and NRL
2, 3, 4, 5	Cameras for TMA experiment	Kyoto Univ. and Clemson Univ.
2, 3, 4, 6	Rocket-beacon receivers	Univ. of Tokyo

Site number and name: 1: Tanegashima-south (TNS), 2: Tanegashima-north (TNN) (Tanegashima Meadow, and Appo Land), 3: Uchinoura (USC), 4: Takazaki, 5: Hata, 6: Tarumizu, 7: Sata, 8: Yamagawa
NiCT: National Institute of Information and Communications Technology (Japan)
NCU: National Central University (Taiwan), NRL: Naval Research Laboratory (USA)

Table 2. Instruments boarded on the sounding rockets S-310-31 and S-310-32 and directing institutes.

Instrument	S-310-31	S-310-32	Institute
Electric Field Detector (EFD)	X		Kyoto Univ. and NASA
Number density of Electrons by Impedance probe (NEI)	X	X	Tohoku Univ.
Plasma and Wave Monitor (PWM)		X	Tohoku Univ.
Fast Langmuir Probe (FLP)	X		ISAS/JAXA
Fixed-Bias Langmuir Probe (FBP)	X		NiCT
Dual-Band Beacon (DBB)	X	X	Kyoto Univ. and NRL
Magnetic Field instrument (MGF)	X	X	Tokai Univ.
Imaging Attitude Finder (IAF)	X	X	Univ. of Tokyo
Tri-Methyl Aluminum release (TMA)		X	Kyoto Univ. and Clemson Univ.

to measure fluctuations of the electron density. Electric fields and electron temperatures were measured using a double-probe instrument (EFD) and a Langmuir probe (FLP) on S-310-31, respectively. A plasma wave receiver (PWM) was installed on S-310-32. Both rockets were equipped with three-dimensional sensitive magnetometers (MGF) for the measurement of both rocket attitude and the geomagnetic field fluctuations. For both rockets, the imaging attitude finder (IAF) was used for accurate measurement of the rocket attitude based on stellar location. We conducted the dual-band beacon (DBB) experiment with both rockets to measure total electron content (TEC) between the rockets and ground-based receivers. The rocket S-310-32 was used mainly for the measurement of wind velocities, as we conducted the TMA (tri-methyl aluminum) release experiment throughout its trajectory above 80 km.

DBB was a unique experiment in SEEK-2, in that the rocket flies between the E_s-layers and the F-region and obtains TEC that belongs only to the E_s-layers. We were able to measure their horizontal structures (Bernhardt et al., 2005). For the DBB experiment, we located receivers at Uchinoura, Tarumizu, Tanegashima-north, and Takazaki (Table 1). To capture the structure and motion of the TMA trail in the E-region and measure wind velocities, four camera sites were located in Uchinoura, Tanegashima-north, Takazaki, and Hata (Table 1).

We installed two portable radars in the Tanegashima-north (TNN) and Tanegashima-south (TNS) sites for SEEK-2. These radars were used to monitor E-region FAI echoes in the rocket observation area and to coordinate the timing of the rocket launches. For that purpose, we networked these sites with USC and monitored behavior of the FAI echoes every night from the rocket range. Other ground-based instruments involved in the SEEK-2 experiments were an operational ionosonde in Yamagawa; three airglow imagers in Sata, Tanegashima-north, and Takazaki; a GPS scintillation receiver in Tarumizu; and the MU radar in Shigaraki. Details are summarized in Table 1.

We used the following criteria for the rocket measurements: no-moon condition, good visibility of TMA releases from at least two of the four ground camera sites, and observation of intense FAI echoes with QP structure with radars in Tanegashima. The first two conditions were requirements from the TMA release experiment, while the last was the most important key for the experiment. On 3 August 2002, at 22:50 JST (13:50 UT; JST=UT+9 h), we found intense FAI echoes from the TNS radar. The range-time intensity (RTI) plot is shown in Fig. 3. The echoes were intense enough and showed clear QP structures. The first rocket, S-310-31, was launched at 23:24 JST (14:24 UT) and reached the altitude of 90 km at 78 s, reached the apogee of 152 km at 194 s, and descended to 90 km at 310 s after launch. The second

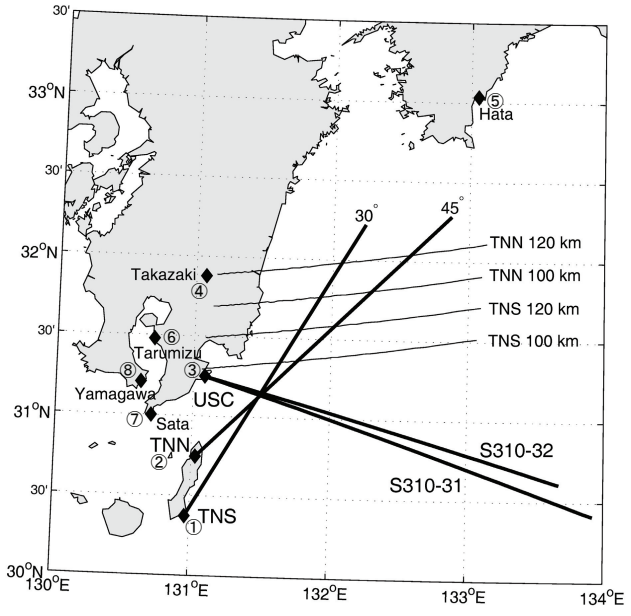

Fig. 2. Observation area of SEEK-2. Trajectories of the sounding rockets S-310-31 and S-310-32 are shown by the curves from USC (Uchinoura Space Center, ISAS/JAXA). Two portable radars were located at TNN (Tanegashima-north) and TNS (Tanegashima-south) sites, and they observed E-region FAI echoes with azimuth angles of 30° and 45°, respectively. Instruments located at the ground sites (1–8) are listed in Table 1.

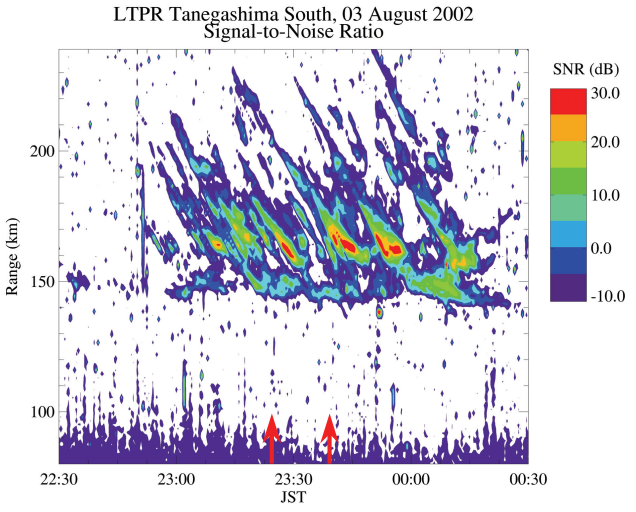

Fig. 3. Range-time intensity (RTI) plot of FAI echoes observed on 3 August 2002. Sounding rockets S-310-31 and S-310-32 were launched at 23:24 JST and 23:39 JST, respectively, as indicated by red arrows (Saito et al., 2005).

rocket, S-310-32, was launched at 23:39 JST (14:39 UT) and reached the altitude of 90 km at 94 s, reached the apogee of 117 km at 170 s, and descended to 90 km at 246 s after launch. The FAI echoes with QP structures were observed using both TNN and TNS radars during 22:50–00:20 JST (13:50–15:20 UT). The timings of the rocket launches are indicated by arrows in Fig. 3.

3 Outline of the results

All measurement instruments on the rockets successfully obtained data. We could operate most of the ground-based cameras for the TMA experiment and beacon receivers for the DBB experiment. Also, two ground-based radars detected clear QP structures in the E-region FAIs. Observations of airglow layers with all-sky imagers, however, were not successful because of cloudy conditions. The ground-based observations continued during the SEEK-2 experiment period in July–August 2002. We summarize the SEEK-2 experiment in this section. For detailed results of each experiment, readers should refer to companion papers in this issue (Bernhardt et al., 2005; Larsen et al., 2005; Maruyama et al., 2005; Ogawa et al., 2005; Onoma et al., 2005; Pfaff et al., 2005; Saito et al., 2005; Wakabayashi et al., 2005; Wakabayashi and Ono, 2005; Yokoyama et al., 2005).

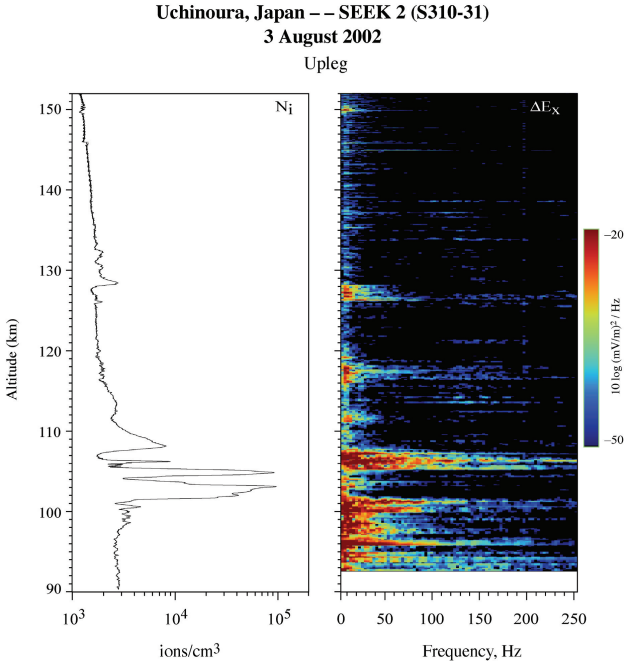

Fig. 4. Spectrograms of one component (E_x) of electric fields from the electric field detector (EFD) (right panel) and plasma-density profile from FBP (left panel) (Pfaff et al., 2005).

3.1 Plasma density of Sporadic-*E* layers

During the SEEK-2 experiment, there were four opportunities for electron-density measurement with two sounding rockets. Height profiles of the electron density were obtained by NEI with both rockets and by FBP with S-310-31 (Wakabayashi et al., 2005). Height differentiation of TEC from the DBB experiment also provided us with density profiles

for both rockets (Bernhardt et al., 2005). In Fig. 4, we show a density profile measured by FBP at the upleg of the rocket S-310-31 (Pfaff et al., 2005). Distribution of electron density throughout the rocket experiment is discussed in detail by Wakabayashi et al. (2005). Throughout the experiment, there were two major peaks of electron density in the E-region, at 102.5 and 104.5 km. Both peaks were clearly recognized as E_s-layers, as they had thicknesses of only 1–2 km. These two peaks were not stable during the experiment since the double-peak structures were seen differently by four rocket passes. The peak at 102.5 km was the major E_s-layer that was seen in all experiments. The peak density of the layer, however, varied from 4.8×10^5 cm^{-3} to 9.0×10^6 cm^{-3}, about a twofold difference. The higher peak at 104.5 km, on the other hand, was detected at the upleg of S-310-31 and at both the upleg and the downleg of S-310-32. Its peak electron densities varied from 4.7×10^5 cm^{-3} to 1.9×10^6 cm^{-3}, an approximately fourfold difference. At the downleg of S-310-31, this peak was missing where the density at the altitude was only 5.5×10^3 cm^{-3}. The plasma was 1/300–1/400 less dense than the measured largest density. The large spatiotemporal variations of the E_s-peaks were confirmed from the findings of the DBB experiment. Bernhardt et al. (2005) successfully obtained the first tomographic imaging of the E_s-layers by analyzing the TEC from Uchinoura and Tarumizu. The analysis retrieved double-layered structures and spatial variability of densities with a horizontal scale of about 30 km. The structured feature of the E_s-layers could be a source of polarization electric fields, as we show below.

In addition to the double-peak structure of the main E_s-layers, several minor density peaks were found from NEI and FBP in a higher region (Wakabayashi et al., 2005). The largest among them was a peak of 7.3×10^3 cm^{-3}, found at 108.1 km in the upleg of S-310-31. There were small but structured density enhancements at 128–132 km, also. As these minor peaks were not persistent through all four NEI measurements, their spatial structures were large. From our experiment, we found that the nighttime E-region was filled with structured E_s-layers at 102–105 km and several minor density peaks above the main E_s-layers.

3.2 Behavior of E-region FAIs (QP echoes)

In July–August 2002, we operated Frequency Agile Radar (FAR) at 24.515 MHz and Lower-Thermosphere Profiler Radar (LTPR) at 31.57 MHz for the TNN and TNS sites, respectively, as shown in Fig. 2. LTPR was capable of locating echoes with interferometry and had a unique feature: It could measure winds by detecting meteor-trail echoes simultaneously during the FAI experiment (Saito et al., 2005). Intense FAI echoes were observed on 3 April 2002, during the rocket experiment by both radars. FAR observed the FAIs from 22:45 JST (13:45 UT) to 00:10 JST (15:15 UT), while LTPR observed them from 23:00 JST (14:00 UT) to 00:30 JST (15:30 UT), as shown in Fig. 3. The RTI plots of both radars similarly showed negative range-rate of the echoes and intermittent behavior, both of which were features satisfactory for the launch conditions. Altitudes of the FAI echoes determined by the radio interferometry with LTPR ranged from 100 to 104 km. It is clear that the radars detected FAI echoes that were associated with the major E_s-layers. Spatial motion of the FAIs determined by interferometry showed that the echoes propagated from east to west at almost constant altitude. Together with the earlier appearance of the echoes with FAR than with LTPR, the structure of the FAI echoes during the rocket experiment was deduced, as shown by the schematic in Fig. 5a. The frontal structure aligned from the north-northeast to the south-southwest and propagated to the west-northwest. Wind velocity from meteor echoes was 52 m/s toward an azimuth angle of $-75°$, which was close to the motion of the frontal structure. From the radar data throughout the observation period, Saito et al. (2005) found typical behavior of QP echoes, as illustrated in Fig. 5b. Phase fronts of the QP structures of FAI echoes typically elongate from the west-northwest to the east-southeast. The direction of the background wind was typically southeast. From LPTR data, they also found that negative (positive) range rate of the QP echoes was associated with southward (northward) wind velocity.

3.3 Electric field, electron temperature, and wind velocity

Electric field was observed with EFD on S-310-31. The electric-field vector was estimated by assuming perpendicularity of the field to the geomagnetic field. Height profile of the field strength and its direction are shown in Fig. 6 (Pfaff et al., 2005). Fluctuating intense electric fields of 3–4 mV/m appeared at an altitude of 95–102 km, where the direction was northwestward. There was another southwestward peak of 5 mV/m at 107–109 km. Above those altitudes, on the other hand, 10- to 15-km-scale wave-like structures remained up to the apogee with amplitudes of 3–5 mV/m, with some excursions to 8–9 mV/m. This field waveform is explained by the mapping along the geomagnetic field from the E_s-layers below (Pfaff et al., 2005). Direction of this slow perturbation was in the northeast-southwest quadrant. In Fig. 4, we show the spectrogram of the electric field from EFD in contrast to the density profile from FBP. Plasma irregularities measured by the electric-field perturbation were enhanced below 108 km where the main E_s-layers existed. Above that region, small but clear enhancements are recognized at altitudes of 113, 118, 128, and 150 km, in association with small local peaks of the plasma density. We will discuss the relationship between these plasma irregularities and E_s-layers in subsect. 4.2. The Langmuir probe (FLP) on S-310-31 observed enhancements of electron temperature at 108, 123, and 128 km, altitudes that were well associated with enhancements of the electric field and the electron densities (Oyama, private communication, 2005).

Neutral-wind velocity was observed by the TMA release experiment with the S-310-32 rocket (Larsen et al., 2005). From Uchinoura, Tanegashima-north, and Hata, they triangulated the TMA trail at 80 km or above. Zonal wind shears

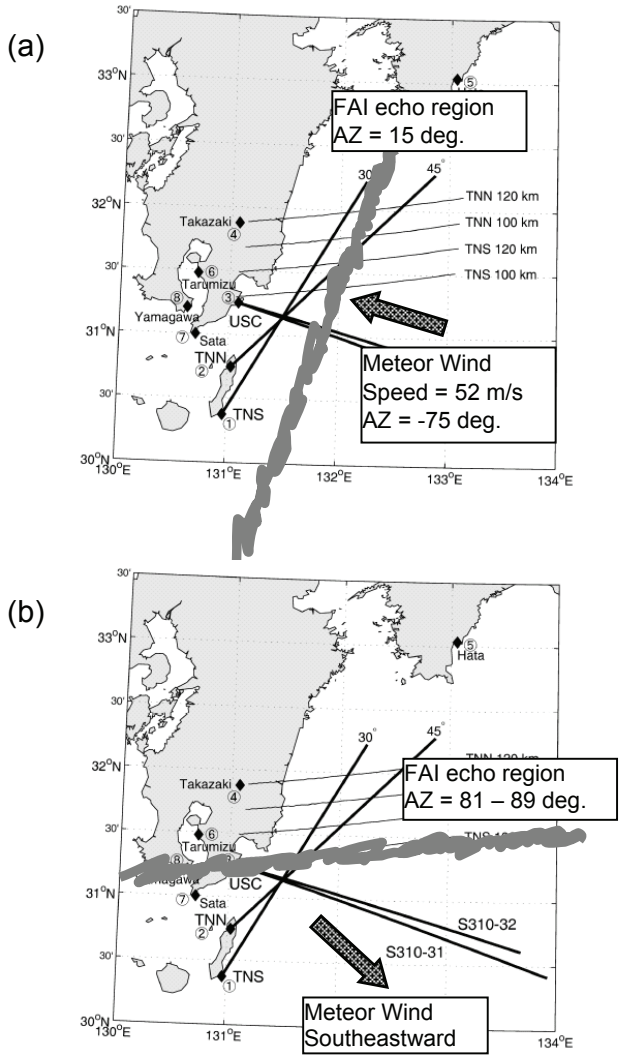

Fig. 5. Alignment of QP echo structures determined from two radar experiments from the TNN and TNS sites. Thick arrows indicate direction of neutral winds. Panel **(a)** shows results during the rocket experiment on 3 August 2002, while panel **(b)** shows the typical structure found from the entire radar observation period (based on Saito et al., 2005).

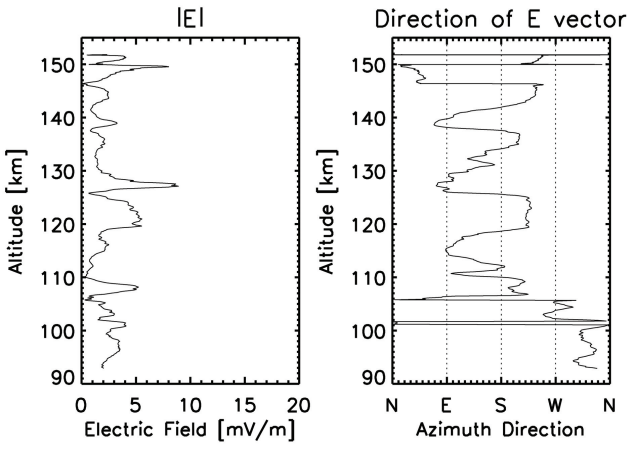

Fig. 6. Height profiles of electric field intensity (left panel) and its direction (right panel) from the electric field detector (EFD) of the S-310-31 rocket upleg (Pfaff et al., 2005).

were detected at 100 and 107 km. These altitudes generally agree with those of two major E_s-layers. The direction of the wind shear was also favorable to ion accumulation. Meridional wind was generally southward but fluctuated above 100 km. The wind vector showed a clockwise rotation with increasing altitudes, which suggested influence of atmospheric waves, such as tides or long-period gravity waves. Onoma et al. (2005) analyzed the propagation of gravity waves by means of an all-sky imager of OI (557.7 nm, at about 96 km altitude) and OH (at about 86 km altitude) airglow. Although simultaneous observations with the SEEK-2 rockets were not successful, the study group found that gravity waves propagated to the southeast when FAI echoes were observed by LTPR. During the SEEK-2 period, Ogawa et al. (2005) continued the MU radar observations and succeeded in simultaneous observations between the MU radar and the airglow imager. As the height of the QP echoes was low, the data were directly compared with the airglow at the same altitude. The group found a positive correlation between height variation of FAI echoes and airglow intensity.

4 Discussion

4.1 Structure of the E-region

To analyze mid-latitude E-region irregularities, we conducted two observation campaigns, SEEK-1 and SEEK-2, by using four sounding rockets: S-310-25, -26, -31, and -32. They were all launched into the E-region with intense FAI echoes. For SEEK-1, two rockets were launched on different nights, whereas for SEEK-2, two rockets were launched on one night, 15 min apart. We compare and contrast these experiments and discuss the structure of the E-region ionosphere with FAIs.

All rockets measured electron density profile with the same instrument. In both SEEK-1 and SEEK-2, we observed E_s-layers with the maximum electron density of about 10^5 cm^{-3} in the height range of 98–105 km. In both campaigns, we conducted TMA-release experiments to measure the neutral winds. We found a good association between the major E_s-layer and intense wind shear. Yokoyama et al. (2005) conducted computer simulations with wind parameters from SEEK-1 and SEEK-2 and confirmed that the E_s-layers were generated by ion accumulation due to wind shear. A common feature of the E_s-layers from both campaigns is large spatial variability of the electron density at the rockets' upleg and downleg. Twice during the four rocket launches, the double-layered E_s-structure in the upleg changed to the single-layered structure in the downleg. Large differences of the peak densities and 1- to 3-km height variations of the

layers were commonly found in SEEK-1 and SEEK-2. Such spatial variability is supported by the ionosonde experiment at Yamagawa, as reported by Maruyama et al. (2005). The DBB experiment more directly showed evidence of spatial structures of the E_s-layers by means of tomographic imaging (Bernhardt et al., 2005).

Another feature common to both SEEK-1 and SEEK-2 is the existence of weak peaks at higher altitudes. All rocket experiments detected several enhancements of electron density of less than $10^5\,\mathrm{cm}^{-3}$ at 110 km or higher. As discussed by Wakabayashi et al. (2005), some of the peaks suggest a layered structure of plasma, but these peaks normally appear more sporadic than the main E_s-layers.

Electric fields measured in SEEK-1 and SEEK-2 exhibit both intense fluctuations around the main E_s-layer and wave-like variations at higher altitudes. However, there are clear differences between the two experiments. In SEEK-1, the intense fluctuations of 10–20 mV/m were found below 130 km, while the intensity of the fluctuation in SEEK-2 was 3–5 mV/m up to 110 km. This difference is attributed to different conditions of the F-region ionosphere due to solar activity. At the time of the rocket launches, F-region peak densities measured by the ionosonde at Yamagawa were $3.2\times10^5\,\mathrm{cm}^{-3}$ (corresponding f_oF_2=5.1 MHz) and $9.6\times10^5\,\mathrm{cm}^{-3}$ (corresponding f_oF_2=8.8 MHz) in SEEK-1 and SEEK-2, respectively. Maximum electron density of E_s-layers, on the other hand, was similar between them. Yokoyama et al. (2005) simulated the E-region ionosphere during the SEEK-2 experiment and found that a polarization electric field of 5.5 mV/m could be induced by a strong neutral wind and horizontal variability of the main E_s-layer, a finding consistent with the results of the rocket experiment. Yokoyama et al. (2004a) previously showed that the intensity of the polarization electric field varies with the plasma density in the F-region ionosphere. When F-region plasma is less dense, the induced polarization electric field is stronger and the mapping effect of the electric field along the geomagnetic field is more enhanced. We understand that the finding of a more intense electric field and its fluctuations of up to 130 km in SEEK-1 is consistent with the simulation results of Yokoyama et al. (2004a). They also find that the E-region plasma above the E_s-layers is accumulated by the polarization electric field that maps along the geomagnetic field. This finding explains the generation of minor density peaks that were detected at 110 km or higher by the rocket experiments.

4.2 FAI association with E_s-layers

E-region FAIs are measured as fluctuations of electric field and/or plasma density by instruments on sounding rockets. In SEEK-1 and SEEK-2, we conducted simultaneous measurements of plasma density profile and the electric-field spectrogram with the same instruments, FBP and EFD, respectively (Pfaff et al., 1998, 2005). As E-region FAIs are generated primarily by the gradient-drift instability, it is possible to evaluate the growth rate from the measured density gradient and the electric-field data. In SEEK-1, the plasma waves were most enhanced at the main E_s-layer at 103 km. Enhancements of the plasma waves were located at 101 and 104 km and were well associated with the positive growth rate. Ground-based radar observations also showed the double-layered structure of the FAI echoes, a finding consistent with results of the rocket experiment (Yamamoto et al., 1998). The gradient-drift instabilities observed in SEEK-1 were thus simply explained in that they were driven by the DC electric field applied to the sharp gradient of E_s-layers. Results of the same experiment in SEEK-2, however, were very different from SEEK-1. As shown in Fig. 4, plasma waves in SEEK-2 were enhanced below 110 km. The relationship between the plasma-wave enhancement and instability growth rate from measured plasma densities and electric fields, however, was not consistent at all, especially in the upleg (Pfaff et al., 2005). That association was consistent only at the topside of the main E_s-layer in the downleg (not shown in Fig. 4). Considering the large spatial variability of the E_s-layer structures in SEEK-2, Pfaff et al. (2005) concluded that the gradient-drift instability associated with neutral winds and horizontal plasma density gradients are necessary to fully explain the plasma wave generation observed in data for SEEK-2. Rigorous proof of these effects would be a task for future studies, as observations of local neutral winds and/or horizontal gradients of plasma density with finer resolutions were missing even in SEEK-2. Other interesting features from the SEEK-2 results are several plasma-wave enhancements and associated local density fluctuations above the main E_s-layers (i.e. at 112, 127, 128, and 148 km in Fig. 4). Taken together with the MU radar observations of FAI echoes as high as 120 km (Yamamoto et al., 1994), these results support upward mapping of the polarization electric field and modification of upper E-region plasma that was proposed by Maruyama et al. (2000) and simulated by Yokoyama et al. (2003).

4.3 Source of QP echoes

Why do QP echoes appear in the radar data? We now discuss what we can determine from the SEEK-2 results. As shown by Saito et al. (2005), the FAI echoes appeared horizontally at nearly constant altitude of around 105 km, which was well associated with the E_s-layers. At the same time, we observed the horizontal variability of the layers (e.g. Bernhardt et al., 2005). Maruyama et al. (2005) carefully analyzed time variation of $\Delta f = f_oE_s - f_bE_s$ from Yamagawa ionosonde and found approximately 10-min variations of Δf that are similar to the periodicity of the QP echoes. The value of Δf first fluctuated in small amplitude for a couple of cycles (for 50–60 min) and then grew very fast. This abrupt increase in Δf was well associated with the QP echo onset. As discussed above, intense plasma waves distributed around heights of the main E_s-layers. Polarization electric fields are induced by the density variability and the neutral winds. From these results, we can conclude that the QP echoes reflect the spatial structures of the main E_s-layers.

One unresolved aspect of the QP echoes is the source of such horizontal structures. In the neutral atmosphere, there are two candidates: gravity waves and KHI. The horizontal structure of the QP echoes during the rocket experiment is shown in Fig. 5a (Saito et al., 2005). Larsen et al. (2005) show that the wind shear in the altitude region was intense enough for shear instability. If zonal wind shear that forms the main E_s-layers could generate KHI, its billow structure would be aligned primarily north-south. KHI is thus plausible to account for the QP structure, as determined in the rocket experiment. Quasi-periodicity of the echoes would be associated with the west-northwestward propagation of the horizontal structures along the background wind. From statistical studies with radars and airglow imagers, on the other hand, we found that typical alignment of QP-echo structures was northeast-southwest, as shown in Fig. 5b (Saito et al., 2005), and southeastward-propagating gravity waves prevailed in association with QP echoes (Onoma et al., 2005). These results are favorable for accepting gravity waves as the source. Computer simulation by Yokoyama et al. (2004b) showed that gravity waves reaching the E-region from the lower atmosphere modulate the main E_s-layer and induce polarization electric fields and FAIs. These two sources, gravity waves and KHI, are very difficult to distinguish. Above the mesopause altitudes, gravity waves are almost always undergoing dissipation, and KHI is one of the major processes of the wave breaking (Yamamoto et al., 1987).

Cosgrove and Tsunoda (2002, 2003) have proposed that there is an azimuth-dependent E_s-layer instability in the mid-latitude E-region. Tsunoda et al. (2004) recently studied the possibility of this mechanism and found reasonable evidence for such instability from published observational results. One of its key features is that the frontal structures of the FAIs should preferably be elongated from northwest to southeast. The estimated QP structures, unfortunately, did not show favorable alignment for this mechanism. In our electric field data, Pfaff et al. (2005) found large-scale perturbations in the northeast-southwest direction. This finding may imply the existence of an azimuth-dependent instability process within the elongated QP structures, conditions under which the elongated QP structure would be modulated more into smaller patches. We conclude from the SEEK-2 data that, among the three candidates for the source of the QP echoes, KHI or gravity waves are the most likely.

Hysell et al. (2004) recently reported excellent results from simultaneous observations with Arecibo IS radar and a 30-MHz imaging radar. The plasma density distribution from the Arecibo IS radar clearly shows that E_s-layers are disturbed by the appearance of FAI echoes. In the RTI plot, a single E_s-layer suddenly became patchy, and several vertical structures started to stretch upward from the E_s-layer. Although the height (range) extent of the stretched structures was small (at most 5–6 km long), the situation resembles the schematic by Ogawa et al. (2002) (here shown in Fig. 1). For horizontal structures of the QP echoes, they used the imaging radar technique and found that the southwest-propagating structures elongated from northwest to southeast. This finding is favorable alignment for the azimuth-dependent instability process. In their paper, they suggested KHI as the source of the QP structures but reached no clear conclusion.

Before SEEK-2, we had a schematic view of the QP echoes, as shown in Fig. 1. From the results shown above, we know that most FAI echoes are associated with horizontally structured E_s-layers around 105 km. We showed that KHI or gravity waves might account for the SEEK-2 data. Above that height, mapping of the polarization electric field along the geomagnetic field was seen from the wave-like variations of the electric field data in the upper E-region. From several small density enhancements seen above 110 km, we found that plasma accumulation owing to the mapped electric field occurs. Our predictions of these phenomena before SEEK-2 were correct. Structures of the E-region above the main E_s-layer, however, were much more sporadic than we expected. Using the portable radars, we did not find many FAI echoes above the main E_s-layer (Saito et al., 2005). The MU radar can observe FAI echoes from higher altitudes than for the main E_s-layers. As shown in Fig. 4, there were several plasma-wave enhancements detected above the main E_s-layers, which should be evidence of FAIs in higher altitudes. The portable radars in SEEK-2 could not detect echoes from the FAIs in the higher region because of the limited sensitivity. The FAIs in higher altitudes exist, but they might not contribute much to the formation of QP structures. This finding differs from our expectations before the SEEK-2 experiment.

5 Conclusions

In conclusion, we summarize findings from the SEEK-1 and SEEK-2 experiments. First, we confirmed that the QP echoes are associated with E_s-layers mainly around 105 km. Accumulation of the E-region plasma into the layers is well explained by the shear of the neutral wind. The E_s-layers are spatially modulated by the motion of the neutral atmosphere, and then FAI echoes start to appear. The sources of the FAIs are the plasma-density gradient of the E_s-layers and the polarization electric field induced by the neutral wind and the spatial inhomogeneity of the E_s-layers. At the main E_s-layer, generation of FAIs is complicated, and wind-driven gradient-driven instability seems effective. The induced-polarization electric field maps along the geomagnetic field and generates small plasma structures above the E_s-layers. In these secondary plasma enhancements, weak FAIs are driven by the polarization electric field. The scenario of the mid-latitude E-region with QP echoes is now clear, thus far. The sources of the QP echoes in the main E_s-layers, especially the mechanism that determines the horizontal structures, can be gravity waves or KHI in the neutral atmosphere, or azimuth-dependent E-region instability of the plasma. From the QP structure in SEEK-2, gravity waves and KHI were more plausible sources than the E_s-instability. The structure alignment in SEEK-2, however, was not very typical compared with many other experimental results (e.g. Tsunoda et al., 2004). The source of QP echo generation

is thus still in discussion. The complicated spatial structure of the E_s-layers that we found from SEEK-2 may imply a competing combination of all processes in the mid-latitude E-region.

Polarization electric fields play an important role in determining the dynamics of the E-region ionosphere, even in the mid-latitude region. Our findings from SEEK-1 and SEEK-2 reminded us of this very basic knowledge. Electric fields with scale sizes of several kilometers or more can easily map to the F-region along the geomagnetic field. Ionospheric E/F-region coupling would be the next interesting research topic. Otsuka et al. (2004) recently observed middle-scale traveling ionospheric disturbance (MS-TID) in geomagnetic conjugate points in Japan and Australia, and found close conjugacy between MS-TIDs in two regions. The finding of the electrodynamic coupling of both hemispheres enhances the importance of studying interactions between plasma and neutral atmosphere and remote coupling of ionospheric regions through polarization electric fields. Studying the source of the QP echoes should be done in such larger frameworks in future studies.

Acknowledgements. The rocket experiment of the SEEK-2 project was supported and conducted by ISAS/JAXA. This study was partly supported by a grant-in-aid for scientific research B (2) (14340145) by the Ministry of Education, Culture, Sports, Science, and Technology (MEXT), Japan.

We express sincere thanks to Nishinoomote City, Takazaki Town, and Kochi-Prefecture Hata Youth-House for providing us with locations for ground-based experiments (i.e. radars, imagers, cameras, and receivers).

Topical Editor M. Pinnock thanks C.-J. Pan and another referee for their help in evaluating this paper.

References

Bernhardt, P. A.: The modulation of sporadic E-layers by Kelvin-Helmholtz billows in the neutral atmosphere, J. Atmos. Solar-Terr. Phys., 64, 1487–1504, 2002.

Bernhardt, P. A., Selcher, C. A., Siefring, C., Wilkens, M., Compton, C., Bust, G., Yamamoto, M., Fukao, S., Ono, T., Wakabayashi, M., and Mori, H.: Radio tomographic imaging of sporadic E-layers during SEEK2, Ann. Geophys., 23, 2357–2368, 2005.

Chau, J. L., Woodman, R. F., and Flores, L A.: Statistical characteristics of low-latitude ionospheric field-aligned irregularities obtained with the Piura VHF radar Source, Ann. Geophys., 20, 8, 1203–1212, 2002,
SRef-ID: 1432-0576/ag/2002-20-1203.

Cosgrove, R. B. and Tsunoda, R. T.: A direction-dependent instability of sporadic E-layers in the nighttime mid-latitude ionosphere, Geophys. Res. Lett., 29, 18, 1864, doi:10.1029/2002GL014669, 2002.

Cosgrove, R. B. and Tsunoda, R. T.: Simulation of the nonlinear evolution of the sporadic E-layer instability in the nighttime mid-latitude ionosphere, J. Geophys. Res., 108(A7), 1283, doi:10.1029/2002JA009728, 2003.

Ecklund, W. L., Carter, D. A., and Balsley, B. B.: Gradient drift irregularities in mid-latitude sporadic-E, J. Geophys. Res., 86, 858–862, 1981.

Fukao, S., Kelley, M. C., Shirakawa, T., Takami, T., Yamamoto, M., Tsuda, T., and Kato, S.: Turbulent upwelling of the mid-latitude ionosphere: 1. Observational results by the MU radar, J. Geophys. Res., 96, 3725–3746, 1991.

Fukao, S., Yamamoto, M., Tsunoda, R. T., Hayakawa, H., and Mukai, T.: The SEEK (Sporadic-E Experiment over Kyushu) campaign, Geophys. Res. Lett., 25, 1761–1764, 1998.

Fukao, S., Hashiguchi, H., Yamamoto, M., Tsuda, T., Nakamura, T., Yamamoto, M. K., Sato, T., Hagio, M., and Yabugaki, Y.: The Equatorial Atmosphere Radar (EAR): System description and first results, Radio Sci., 38, 4, 1053, doi:10.1029/2002RS002767, 2003.

Haldoupis, C., Schlegel, K., and Farley, D. T.: An explanation for type 1 radar echoes from the mid-latitude E-region ionosphere, Geophys. Res. Lett., 23, 97–100, 1996.

Hysell, D. L. and Burcham, J. D.: The 30-MHz radar interferometer studies of mid-latitude E-region irregularities, J. Geophys. Res., 105, 12 797–12 812, 2000.

Hysell, D. L., Yamamoto, M., and Fukao, S.: Imaging radar observations and theory of type I and type II quasiperiodic echoes, J. Geophys. Res., 107(A11), 1360, doi:10.1029/2002JA009292, 2002.

Hysell, D. L., Larsen, M. F., and Zhou, Q. H.: Common volume coherent and incoherent scatter radar observations of mid-latitude sporadic E-layers and QP echoes, Ann. Geophys., 22 (9), 3277–3290, 2004,
SRef-ID: 1432-0576/ag/2004-22-3277.

Kagan, L. M. and Kelley, M. C.: A wind-driven gradient drift mechanism for mid-latitude E-region ionospheric irregularities, Geophys. Res. Lett., 25, 4141–4144, 1998.

Larsen, M. F., Fukao, S., Yamamoto, M., Tsunoda, R., Igarashi, K., and Ono, T.: The SEEK chemical release experiment: Observed neutral wind profile in a region of sporadic E, Geophys. Res. Lett., 25, 1789–1792, 1998.

Larsen, M. F.: A shear instability seeding mechanism for quasi-periodic radar echoes, J. Geophys. Res., 105, 24 931–24 940, 2000.

Larsen, M. F., Yamamoto, M., Fukao, S., Saito, A., and Tsunoda, R. T.: SEEK 2: Observations of neutral winds, wind shears, and wave structure during a sporadic E/QP-event, Ann. Geophys., 23, 2369–2375, 2005.

Maruyama, T., Fukao, S., and Yamamoto, M.: A possible mechanism for echo-striation generation of radar backscatter from mid-latitude sporadic E, Radio Sci., 35, 1155–1164, 2000.

Maruyama, T., Saito, S., Yamamoto, M., and Fukao, S.: Simultaneous observation of sporadic E by rapid-run ionosonde and coherent VHF radar during SEEK-2, Ann. Geophys., accepted, 2005.

Nakamura, M., Noda, H., Yoshikawa, I., and Iwagami, N.: DC electric field measurement in the SEEK campaign, Geophys. Res. Lett., 25, 1777–1780, 1998.

Ogawa, T., Takahashi, O., Otsuka, Y., Nozaki, K., Yamamoto, M., and Kita, K.: Simultaneous middle and upper atmosphere radar and ionospheric sounder observations of mid-latitude E-region irregularities and sporadic E-layer, J. Geophys. Res., 107(A10), 1275, doi:10.1029/2001JA900176, 2002.

Ogawa, T., Otsuka, Y., Onoma, F., Shiokawa, K., and Yamamoto, M.: Relationship between E-region field-aligned quasi-periodic radar echoes and lower thermospheric dynamics, Ann. Geophys., 23, 2391–2399, 2005.

Onoma, F., Otsuka, Y., Shiokawa, K., Ogawa, T., Yamamoto, M., Fukao, S., and Saito, S.: Relationship between gravity waves in

OH and OI airglow images and VHF radar backscatter from E-region field-aligned irregularities during the SEEK-2 campaign, Ann. Geophys., 23, 2385–2390, 2005.

Otsuka, Y., Shiokawa, K., Ogawa, T., and Wilkinson, P.: Geomagnetic conjugate observations of medium-scale traveling ionospheric disturbances at mid-latitude using all-sky airglow imagers, Geophys. Res. Lett., 31, L15803, doi:10.1029/2004GL020262, 2004.

Pan, C. J. and Rao, P. B.: Low altitude quasi-periodic radar echoes observed by the Gadanki VHF radar, Geophys. Res. Lett., 29(11), Art. No. 1530, 2002.

Perkins, F. W.: Spread *F* and ionospheric currents, J. Geophys. Res., 78, 218–226, 1973.

Pfaff, R., Yamamoto, M., Marionni, P., Mori, H., and Fukao, S.: Electric field measurements above and within a sporadic E-layer, Geophys. Res. Lett., 25, 1769–1772, 1998.

Pfaff, R. F., Freudenreich, H., Yokoyama, T., Yamamoto, M., Fukao, S., and Mori, H.: Electric field measurements of DC and long wavelength structures associated with sporadic E-layers and QP radar echoes, Ann. Geophys., 23, 2319–2334, 2005.

Rao P. B., Yamamoto, M., Uchida, A., Hassenpflug, I., and Fukao, S.: MU radar observations of kilometer-scale waves in the mid-latitude lower E-region, Geophys. Res. Lett., 27(22), 3667–3670, 2000.

Riggin, D., Swartz, W. E., Providakes, J., and Farley, D. T.: Radar studies of long-wavelength waves associated with mid-latitude sporadic-E layers, J. Geophys. Res., 91, 8011–8024, 1986.

Rosado-Roman, J. M., Swartz, W. E., and Farley, D. T.: Plasma instabilities observed in the E-region over Arecibo and a proposed nonlocal theory, J. Atmos. Solar-Terr. Phys. 66, 1593–1602, 2004.

Saito, S., Yamamoto, M., Fukao, S., Marumoto, M., and Tsunoda, R. T.: Radar observations of field-aligned plasma irregularities in the SEEK-2 campaign, Ann. Geophys., 23, 2307–2318, 2005.

Seyler, C. E., Rosado-Roman, J. M., and Farley, D. T.: A nonlocal theory of the gradient-drift instability in the ionospheric E-region plasma at mid-latitudes J. Atmos. Solar-Terr. Phys. 66, 1627–1637, 2004.

Tanaka, T. and Venkateswaran, S. V.: Characteristics of field-aligned E-region irregularities over Iioka (36N), Japan-I, J. Atmos. Terr. Phys., 44, 381–393, 1982.

Tsunoda, R. T., Fukao, S., and Yamamoto, M.: On the origin of quasi-periodic radar backscatter from mid-latitude sporadic E, Radio Sci., 29, 349–365, 1994.

Tsunoda, R. T., Fukao, S., Yamamoto, M., and Hamasaki, T.: First 24.5-MHz radar measurements of quasi-periodic backscatter from field-aligned irregularities in mid-latitude sporadic E, Geophys. Res. Lett., 25, 1765–1768, 1998a.

Tsunoda, R. T.: On polarized frontal structures, type-1 and quasi-periodic echoes in mid-latitude sporadic E, Geophys. Res. Lett., 25, 14, 2641–2644, 1998b.

Tsunoda, R. T., Buonocore, J. J., Saito, A., Kishimoto, T., Fukao, S., and Yamamoto, M.: First observations of quasi-periodic radar echoes from Stanford, California, Geophys. Res. Lett., 26, 7, 995–998, 1999.

Tsunoda R. T., Cosgrove, R. B., and Ogawa, T.: Azimuth-dependent E_S layer instability: A missing link found, J. Geophys. Res., 109, A12303, doi:10.1029/2004JA010597, 2004.

Urbina, J., Kudeki, E., Franke, S. J., Gonzalez, S., Zhou, Q. H., and Collins, S. C.: 50 MHz radar observations of mid-latitude E-region irregularities at Camp Santiago, Puerto Rico, Geophys. Res. Lett., 27, 18, 2853–2856, 2000.

Wakabayashi, M. and Ono, T.: Multi layer structure of mid-latitude sporadic E observed during the SEEK-2 campaign, Ann. Geophys., 23, 2347–2355, 2005.

Wakabayashi, M., Ono, T., Mori, H., and Bernhardt, P. A.: Electron density and plasma waves measurement in mid-latitude sporadic E-layer observed during the SEEK-2 campaign, Ann. Geophys., 23, 2335–2345, 2005.

Woodman, R. F., Yamamoto, M., and Fukao, S.: Gravity wave modulations of gradient drift instabilities in mid-latitude sporadic-E irregularities, Geophys. Res. Lett., 18, 1197–1200, 1991.

Yamamoto, M., Tsuda, T., Kato, S., Sato, T., and Fukao, S.: A saturated inertia gravity wave in the mesosphere observed by the middle and upper atmosphere radar, J. Geophys. Res., 92, 11 993–11 999, 1987.

Yamamoto, M., Fukao, S., Woodman, R. F., Ogawa, T., Tsuda, T., and Kato, S.: Mid-latitude E-region field-aligned irregularities observed with the MU radar, J. Geophys. Res., 96, 15 943–15 949, 1991.

Yamamoto, M., Fukao, S., Ogawa, T., Tsuda, T., and Kato, S.: A morphological study on mid-latitude E-region field-aligned irregularities with the MU radar, J. Atmos. Terr. Phys., 54, 769–777, 1992.

Yamamoto, M., Komoda, N., Fukao, S., Tsunoda, R. T., Ogawa, T., and Tsuda, T.: Spatial structure of the E-region field-aligned irregularities revealed by the MU radar, Radio Sci., 29, 337–347, 1994.

Yamamoto, M., Itsuki, T., Kishimoto, T., Tsunoda, R. T., Pfaff, R. F., and Fukao, S.: Comparison of E-region electric fields observed with a sounding rocket and a Doppler radar in the SEEK campaign, Geophys. Res. Lett., 25, 1773–1776, 1998.

Yamamoto, M.-Y., Ono, T., Oya, H., Tsunoda, R. T., Larsen, M. F., Fukao, S., and Yamamoto, M.: Structures in sporadic-E observed with an impedance probe during the SEEK campaign: Comparisons with neutral-wind and radar-echo observations, Geophys. Res. Lett., 25, 1781–1784, 1998.

Yokoyama, T., Yamamoto, M., and Fukao, S.: Computer simulation of polarization electric fields as a source of mid-latitude field-aligned irregularities, J. Geophys. Res., 108(A2), 1054, doi:10.1029/2002JA009513, 2003.

Yokoyama, T., Yamamoto, M., Fukao, S., and Cosgrove, R. B.: Three-dimensional simulation on generation of polarization electric field in the mid-latitude E-region ionosphere, J. Geophys. Res., 109, A01309, doi:10.1029/2003JA010238, 2004a.

Yokoyama, T., Horinouchi, T., Yamamoto, M., and Fukao, S.: Modulation of the mid-latitude ionospheric E-region by atmospheric gravity waves through polarization electric field, J. Geophys. Res., 109, A12307, doi:10.1029/2004JA010508, 2004b.

Yokoyama, T., Yamamoto, M., and Fukao, S.: Numerical simulation of mid-latitude ionospheric E-region based on the SEEK and the SEEK-2 observations, Ann. Geophys., 23, 2377–2384, 2005.